Crystallization and Melting Behavior of Amorphous Poly(iminosebacoyl iminodecamethylene)

SUSHENG TAN,[1,*] AIHUA SU,[2] XIAONIU YANG,[1] ENLE ZHOU[1,*]

[1]Polymer Physics Laboratory, Changchun Institute of Applied Chemistry, Chinese Academy of Sciences, 159 Renmin Street, Changchun, 130022 People's Republic of China

[2]Department of Applied Chemistry, Jilin University of Technology, 142 Renmin Street 130025 Changchun, People's Republic of China

Received 1 August 1999; accepted 10 December 1999

ABSTRACT: Multiple melting behavior was observed in the differential scanning calorimetry (DSC) scans for the isothermally crystallized poly(iminosebacoyl iminodecamethylene) (PA1010) samples. Coexistence of crystal populations with different lamellar thickness in PA1010 was discussed by means of DSC, wide-angle X-ray diffraction (WAXD), and small-angle X-ray scattering techniques. During crystallization of the polymer, a major lamellar crystal population developed first, which possessed a higher melting temperature. However, a small fraction of the polymer formed minor crystal population with thinner lamellae, which was metastable and, upon post-annealing, could grow into more stable and thicker lamellae through melting and recrystallization process. Lamellae insertion or stacks would develop during the post-annealing at a lower temperature for the isothermally crystallized samples; thus, multiple crystal populations with different thickness could be produced. It is the multiple distribution of lamella thickness that gives rise to multiple melting behavior of crystalline polymers.
 J Appl Polym Sci 76: 993–1002, 2000

Key words: PA1010; crystallization; melting; morphology

INTRODUCTION

Polyamide is one class of important engineering plastics, which has a combination of high strength, elasticity, toughness, and abrasion resistance. Poly(iminosebacoyl iminodecamethylene) (PA1010), which is specifically produced commercially in China, is a unique polyamide. The structural formula of PA1010 is represented in Figure 1. In addition to the common features, it has a pronounced resistance to high moisture, as compared with polyamide 6,6. PA1010 made from sebacoyl acid and decamethylene diamide have lower water absorption and, thus, better dimensional stability than the other polyamides. Their lower melting points permit them to be processed in ways not applicable to the other species, for example, fluidized-bed coating. Mo and coworkers[1] report the crystal structure and thermodynamic parameters of PA1010. The PA1010 crystallizes in the triclinic system, with the following lattice dimensions: $a = 0.49$ nm, $b = 0.54$ nm, $c = 2.78$ nm, $\alpha = 49°$, $\beta = 77°$, and $\gamma = 63.5°$. PA1010 crystal contains one monomeric unit in its unit cell and belongs to the $P\bar{1}$ space group.

A multiple-melting phenomenon is observed in many semicrystalline polymers and is given more

Correspondence to: S. Tan.
Contract grant sponsors: National Natural Science Foundation of China and the National Key Projects for Fundamental Research, Macromolecular Condensed State of the State Science and Technology Commission of China.

Journal of Applied Polymer Science, Vol. 76, 993–1002 (2000)

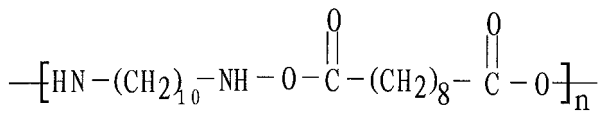

Figure 1 Structural formula of PA1010.

and more attention. The origin of the multiple endothermic peaks is the focus of intense activity in the thermal analysis of polymers. Previously isothermally crystallized poly(ethylene terephthalate) (PET) and poly(aryl ether ether ketone) (PEEK) demonstrate most vividly the effect. In such a case, two endothermic melting peaks are observed in subsequent differential scanning calorimetry (DSC) heating scans; a minor low-temperature peak locates at a few degrees above the prior crystallization temperature in addition to a major high-temperature peak (~250°C for PET and 335°C for PEEK).[2–8] As for polyamides, few of results about the multiple-melting phenomenon have been found in the publications. Recently, we investigated the crystallization and melting behavior of PA1010 to elucidate the morphological variations and stability of its crystalline lamellae. Two or more melting peaks were found in the DSC heating scans of isothermally crystallized samples. Therefore, following the approaches of various workers,[3,5–9] we carried out further experiments to check the morphological changes and the possibility of various origin of double or multiple melting peaks.

EXPERIMENTAL

Sample Preparation

The polymer powder of PA1010, supplied by Shanghai Celluloid Factory, China, were dried at 50°C under reduced pressure for 10 h to withdraw moisture and were then compression-molded at 220°C into sheets with about 0.5 mm thickness and quenched into an ice-water bath to form amorphous samples. For the single-step isothermal crystallization, small pieces were cut from the sheet and were placed on a preheated plate at deferent temperatures for 1 h to allow the sample to crystallize isothermally. In addition, another procedure, the so-called multiple-step-annealing process, was used in this work to investigate the origin of multiple-melting behavior of the crystallized samples. These samples isothermally crystallized at 120°C for 1 h were annealed at higher temperatures, such as 145, 170, and 195°C; or samples isothermally crystallized at 195°C for 1 h were annealed at lower temperatures, such as 170, 145, and 120°C, progressively. To study the sequence of crystallization, the amorphous sheets were isothermally crystallized at 120°C for different periods of time.

DSC Measurements

Thermograms of the samples were obtained with a Perkin–Elmer 7 series thermal analysis system

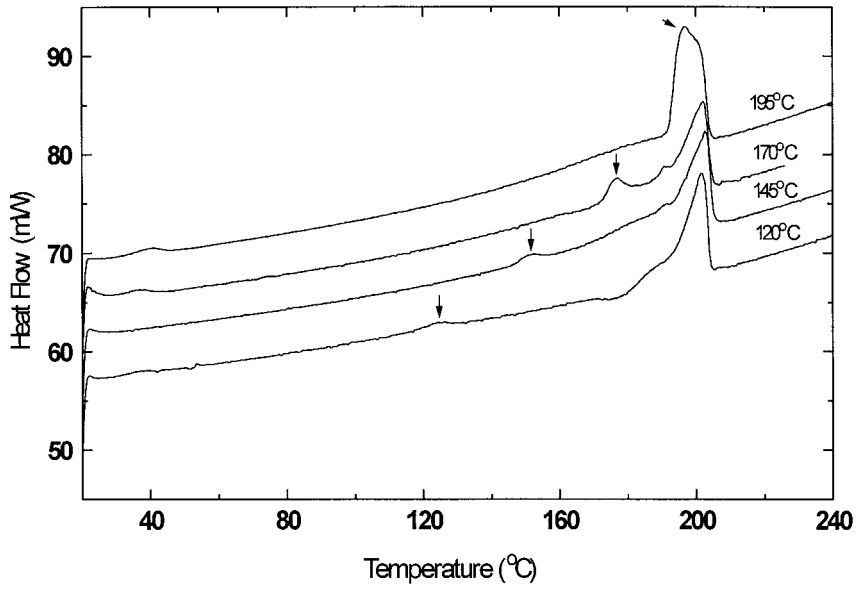

Figure 2 DSC diagrams of PA1010 crystallized at different temperatures for 1 h.

Table I DSC Parameters of PA1010 Isothermally Crystallized from Glassy State at Different Temperatures

	Melting Peak Temperature (°C)		Heat of Fusion (J g)	
T_c (°C)	Lower	Upper	Lower	Upper
120	124	202	3.4	55.5
145	152	203	4.5	68.9
170	178	202	7.2	69.3
195	197	202		88.7

operated in standard DSC mode equipped with a Digital Equipment Corp. (DEC) computer for data acquisition/analysis on 10-mg samples heated at 10°C min. The temperature and heat of melting were calibrated with a high-purity indium standard. A nitrogen purge was provided throughout the DSC scan.

Wide-Angle X-ray Diffraction (WAXD) and Small-Angle X-ray Scattering (SAXS)

The WAXD measurements of the crystallized samples were carried out with a Philips PW1700 Model automatic X-ray diffractometer operated at 40 kV and 30 mA in the reflection mode. The step of 0.02° was used in all scans from 5 ~ 45°. The diffraction peak positions and widths observed from WAXD experiments were carefully calibrated with silicon crystals.

Small-angle X-ray scattering intensities for the post-annealed samples were obtained with the same X-ray apparatus equipped with Kratky small-angle X-ray camera and a sample-to-detector distance of 200 mm. The measurements were performed with a CuKα radiation source. Measured intensities were corrected for background scattering and desmeared with a method proposed by Strobl.[10]

RESULTS

Figure 2 shows the DSC scans of PA1010 samples isothermally crystallized at different temperatures. In addition to the higher-temperature melting peak at about 202°C, a minor, lower-temperature melting peak was observed in all curves. The minor melting peak became stronger and sharper with elevating crystallization temperature. That is to say, the heat of fusion for the minor peak increased with the crystallization temperature elevating. Table I lists the thermal properties for these PA1010 samples.

Figure 3 shows the DSC traces of PA1010 crystallized at 120°C for different period of time. The upper endothermic peak kept nearly invariant. By contrast, the minor lower-temperature melting peak shifted to a higher position with an in-

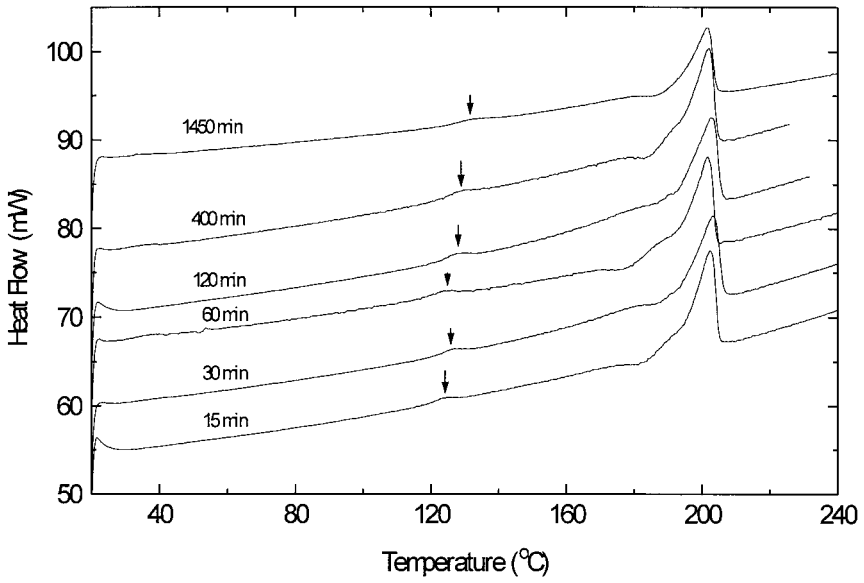

Figure 3 DSC scans at 10°C min of PA1010 crystallized at 120°C for different times.

Table II DSC Parameters of PA1010 Isothermally Crystallized at 120°C for Different Periods of Time

	Melting Peak Temperature (°C)		Heat of Fusion (J g)	
t_c (min)	Lower	Upper	Lower	Upper
15	124	202	1.2	57.9
30	127	203	1.8	61.1
60	124	202	3.4	55.5
120	128	203	3.0	63.4
400	130	202	3.4	54.7
1450	131	202	3.6	60.0

crease in the period of annealing; and the heat of fusion for the minor lower temperature peak also increased with the annealing time. This may be attributed to the perfection and/or thickening of the thinner lamellar crystals produced between the existing main lamellae.[8] Thermal properties for this series of PA1010 samples are listed in Table II.

In Figure 4 are the DSC thermograms for PA1010 crystallized at 160°C for 24 h and then scanned at 20°C/min. In this figure, two scanning methods were used to study the possible origin of the minor lower-temperature melting peak that was produced by the isothermal crystallization or annealing. Curve (A) in Figure 4 represents the heating scan, which ranged from 20 to 240°C; two endothermic peaks were observed clearly as other isothermally crystallized samples. It is clear that the lower-temperature melting peak located at 176°C and the upper endothermic peak appeared at ~ 196°C. The heat of fusion for the lower-temperature peak was 25 J/g, and that for the upper endothermic peak was 76 J/g. Curve (B) in Figure 4 shows the heating scan at the same rate of 20°C min from 20 to 182°C, from which a partially melting peak was identified at 176°C with the heat of fusion of ~19 J/g. Curve (C) in Figure 4 represents the immediate heating scan for the quenched sample from 182 to 150°C in liquid nitrogen; the scanning range is from 150 to 240°C. We saw a shoulder peak at approximately 186°C near the main upper endothermic peak. According to the fitting analysis, the shoulder peak may comes from overlapping of the minor lower-temperature melting peak (176°C, partially melted during the first scan) and the main upper endothermic peak. The total heat of fusion during this scan is 83 J/g. The heat of fusion of ~ 7 J/g for melting of the remaining lamellae during the first scan from 20 to 182°C could be subtracted from that of the main melting peak. No recrystallization exothermal peak was identified.

Figure 5 shows the DSC curves for PA1010 first crystallized at 120°C and then progressively

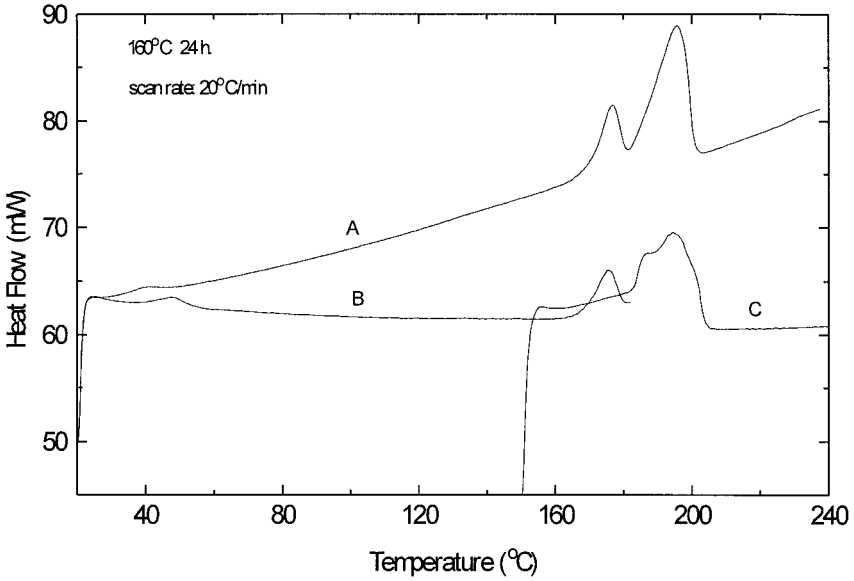

Figure 4 Thermograms of DSC heating scans for PA1010 crystallized at 160°C for 24 h: (A) scanned from 20 to 240°C; (B) scanned from 20 to 182°C and quenched to 150°C, then (C) scanned again from 150 to 240°C.

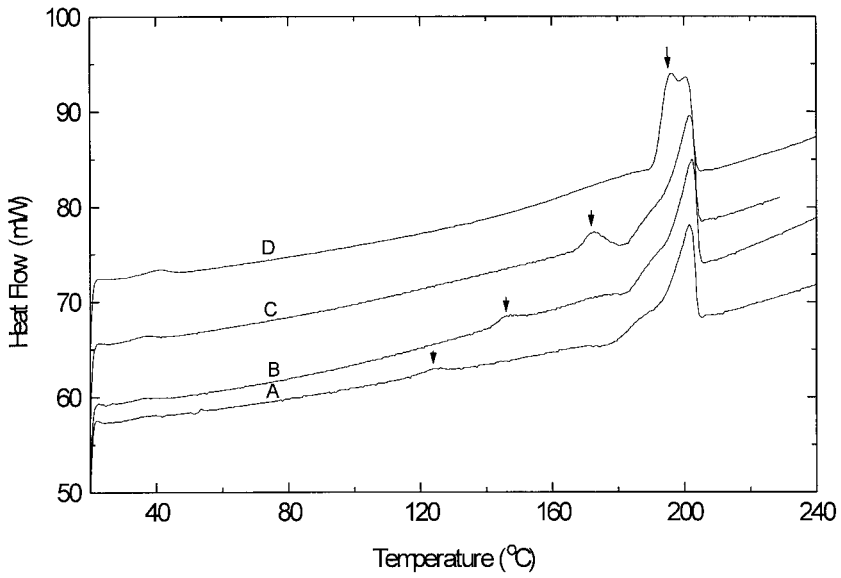

Figure 5 DSC curves of PA1010 crystallized first at 120°C (A) and then annealed progressively at (B) 145°C; (C) 145 and 170°C; and (D) 145, 170, and 195°C.

annealed at 145, 170, and 195°C. In any case, only two melting peaks were observed. The higher endothermic peak kept almost invariant. In contrast, the minor lower-temperature melting peak shifted to a higher temperature with stepwise elevation of the annealing temperature; and the heat of fusion of this minor peak also increased (see Table III). It is obvious that the thinner lamellae formed at lower crystallization temperature melted during the later annealing at higher temperature and then transformed to thicker lamellae. When the annealing temperature was near the upper melting temperature, such as 195°C, we still identified two melting peaks from the DSC heating scan [Fig. 5, curve (D)], which demonstrated the melting of two separated crystal populations with different perfection.

Table III DSC Parameters of PA1010 Subjected to Multiple Step Post-annealing

Crystallized and Then Sequentially Annealed Sample	Melting Peak Temperature (°C)		Heat of Fusion (J g)	
	Lower	Upper	Lower	Upper
Crystallized at 120°C	124	202	3.4	55.5
Annealed at 145°C	147	202	10.6	54.6
Annealed at 170°C	173	202	10.3	56.6
Annealed at 195°C	196	201		87.6

DSC thermograms of PA1010 first crystallized at 195°C and then stepwise annealed at 170, 145, and 120°C are shown in Figure 6. The control crystallized sample displayed a broad melting peak [Fig. 6, curve (a)], which was attributed to the overlapping of a minor endothermic peak and a main melting peak. After stepwise annealing the sample at lower temperatures, we saw that the samples showed multiple melting peaks in their DSC heating scans. The number of endothermic peaks increased with that of annealing steps. The thermal properties for these samples are listed in Table IV.

Figures 7 and 8 illustrate the WAXD diagrams for the two series of post-annealed PA1010 samples. Besides the sharpening of those diffraction peaks, which showed that the crystallinity increased with the post-annealing, there were no different peaks that represented other crystal forms. The crystallinities calculated by this method are shown in Table V. There was a systematic increase in crystallinity with increasing the annealing steps.

Figures 9 and 10 show the SAXS curves for two series of post-annealed PA1010 samples. The cal-

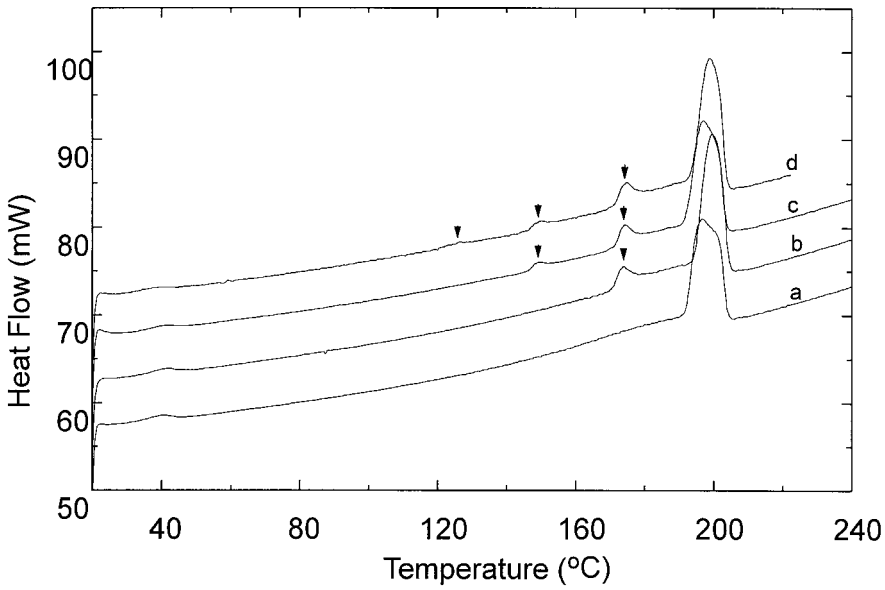

Figure 6 DSC thermograms of PA1010 crystallized first at 195°C (a) and then annealed stepwise at (b) 170°C; (c) 170 and 145°C; and (d) 170, 145, and 120°C.

culated long period of the samples according to the Bragg's equation are listed in Table V. The long period varied with the post-annealing.

DISCUSSION

Melting and Its Origin

Double- or multiple-melting behavior is observed in many semicrystalline polymers, such as PET and PEEK. Five models, which can be grouped into two hypotheses, are proposed to explain the origin of the two endothermic peaks. One hypothesis illustrates that the peaks are related to two distinct crystalline morphologies, which can be attributed to lamellar insertion and/or lamellar stacks, etc.[5,8,9,11–14] The other demonstrates that the peaks are associated to a melting and recrystallization phenomenon of one initial crystal morphology. According to this model, the lower melting peak is indicative of the onset of melting of characteristic lamellar crystals. In the interval between the two peaks, all the molecules experience a continuous melting and recrystallization process during DSC heating scan. Anyway, the lower endothermic peak represents the melting of metastable crystal population.

The double melting phenomena shown by PA1010 might represent different populations relevant to the history of the sample. The upper melting peak represented the melting of the main thicker lamellar populations, which were produced at the whole annealing process by primary crystallization; and the lower endothermic peak represented the melting of the thinner lamellar populations, which formed at the later stage by secondary crystallization. The former was almost independent upon the crystallization tempera-

Table IV DSC Parameters of PA1010 Subjected to Multiple Step Post-annealing

Crystallized and then Sequentially Annealed Sample	Melting Peak Temperature (°C)				Heat of Fusion (J g)			
	L1	L2	L3	Upper	L1	L2	L3	Upper
Crystallized at 195°C			197	202				88.7
Annealed at 170°C			174	199			9.1	84.8
Annealed at 145°C		149	175	197		2.8	10.2	82.4
Annealed at 120°C	126	150	175	199	2.3	3.7	11.1	77.5

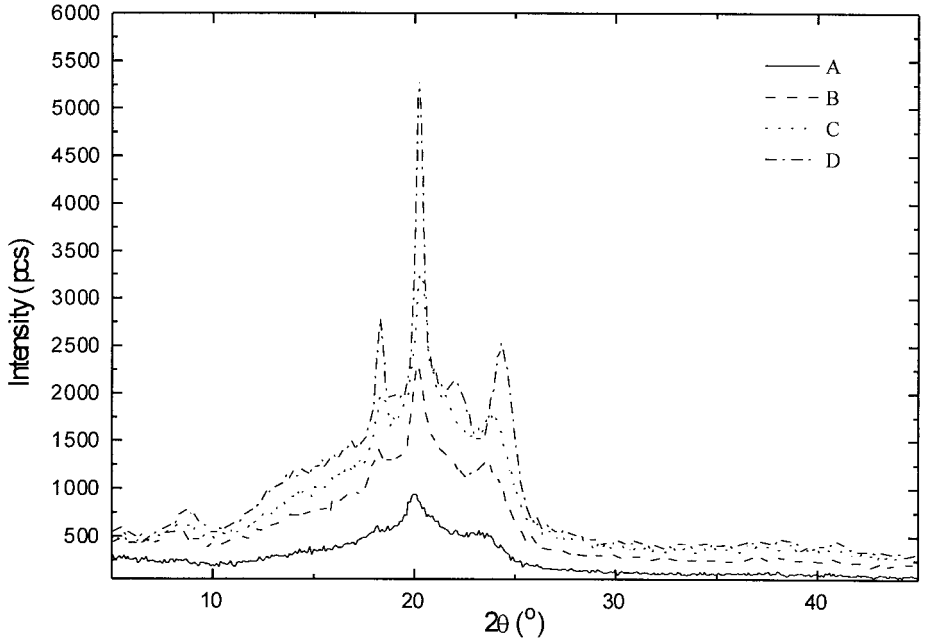

Figure 7 WAXD patterns of PA1010, which were subjected to isothermal crystallization at 120°C for 1 h (A) and then annealing at (B) 145°C for 1 h; (C) 145 and 170°C for 1 h, respectively; and (D) 145, 170, and 195°C for 1 h, respectively.

ture and crystallization time. That is to say the heat of fusion of the main melting peak kept almost invariant with increasing crystallization temperature (see Fig. 2 and Table I) and crystallization time (as shown in Fig. 3 and Table II). The secondary population is strongly dependent

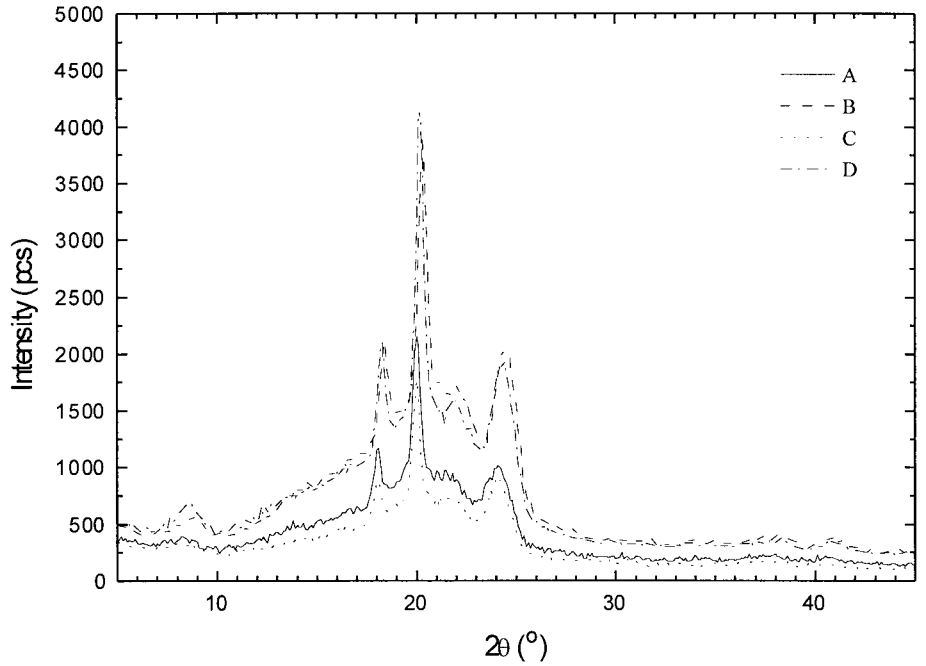

Figure 8 WAXD patterns of PA1010, which were subjected to isothermal crystallization at 195°C for 1 h (a) and then annealing at (b) 170°C for 1 h; (c) 170 and 145°C for 1 h, respectively; and (d). 170, 145, and 120°C for 1 h, respectively.

Table V Long Period and Crystallinity for the Post-Annealed PA1010 Samples

Samples	Long Period (nm)	Crystallinity (%)	Samples	Long Period (nm)	Crystallinity (%)
Crystallized at 120°C	8.3	27.2	crystallized at 195°C	12.5	29.5
Annealed at 145°C	9.1	28.5	annealed at 170°C	11.7	30.2
Annealed at 170°C	10.0	29.2	annealed at 145°C	10.5	31.1
Annealed at 195°C	11.7	31.4	annealed at 120°C	9.5	31.8

upon the crystallization temperature, especially on the time of crystallization or annealing. As shown in Figure 3, the lower endothermic peak became sharper, and the enthalpy of melting (see Table II) was larger with increasing crystallization time, which shows that the secondary lamellar population developed and gave a prominently slightly higher peak with time. During secondary crystallization, the polymers crystallize as metastable lamellae that have melting points depressed because of their large surface-to-volume ratios and the high surface-free enthalpies of their folded surfaces.[15–17]

Another test of the origin of double melting peaks was illustrated in Figure 4. Here, the sample was crystallized from the glassy state at 160°C for 24 h. After scanning from 20 to 182°C at the same heating rate, we saw that the sample exhibited no recrystallization process in the reheating scan from 152 to 240°C, as shown by curve (C) in Figure 4. This was a supplement for the populations of lamellae with different thickness.

The fraction of crystals formed during isothermal crystallization was determined. In the temperature range used here, the crystallinity slightly increased with post-annealing. The area under the small endotherm above the crystallization temperature was too small to account for melting of this crystal fraction, whereas very good agreement was obtained with the crystal fraction determined from the upper temperature endotherm. Crystallization was very rapid in the temperature range used

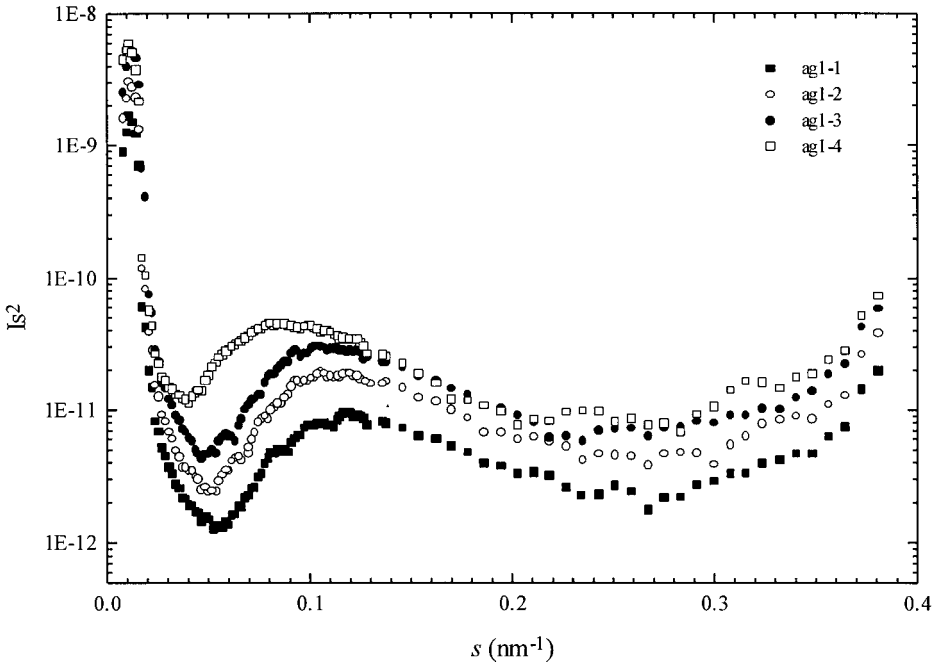

Figure 9 Lorentz-corrected SAXS intensity for the post-annealed PA1010 with the same history as shown in Figure 4. For the sake of clarity, the data points were shifted upwards.

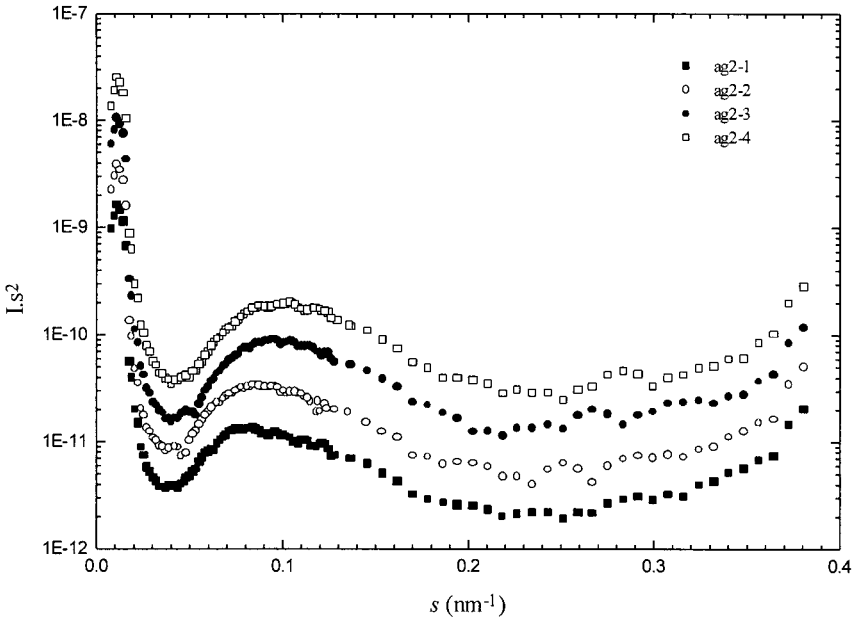

Figure 10 Lorentz-corrected SAXS intensity for the post-annealed PA1010 with the same history as shown in Figure 5. For the sake of clarity, the data points were shifted upwards.

here; hence, additional crystallization or secondary crystallization may occur in the samples through formation of small, imperfect crystals between existing main lamellae. These crystals would be metastable and would melt just above their formation temperature, which gave rise to a small endothermic response.

Further evidence is given by SAXS experiments. Long periods can be determined after the Lorentz correction of the background-corrected scattering intensity. Table V lists the long periods of PA1010 crystallized at 120°C and post-annealed at different higher temperatures. It is found that after post-annealing, the long period showed a clear increase as compared with the initial one. One possible explanation is the melting of the thermodynamically less stable, thinner lamellae in-between the more stable, thicker lamellae. Consequently, the residual thicker lamellae increase the long period.[8]

Recrystallization Upon Post-annealing

The stepwise crystallization (see Fig. 5 and Table III) showed that the low-melting peak accounted for the melting of the secondary lamellar population; the perfection of the metastable crystals was limited by the already existing main crystal population. The lower minor DSC peak accordingly marked the point at which the original isothermally formed crystals became unstable and the melting occurred. If the heating process was interrupted and stayed at this interrupted temperature for enough time, another crystal population with greater stability than the original thinner lamellae would form. During subsequent reheating, we saw that the melting process recommenced and was marked by another minor endothermic peak at a corresponding higher temperature, as seen in the post-annealed samples. It is clear that melting and recrystallization occurred during the post-annealing process. The main endothermic peak was almost constant for those post-annealed samples, which means that the thickening or perfection of the main crystal population undergoes very slowly.

Lamellar Insertion on Post-annealing

As discussed above, the low endothermic peak is attributed to the melting of the metastable crystal population formed at the secondary crystallization stage. Other lower-temperature melting peaks were observed if we have annealed the crystallized sample at other lower temperatures than the original crystallized temperature. Figure 6 and Table IV show the DSC scans of four PA1010 samples, which were progressively crys-

tallized at each indicated lower temperature for 60 min. The more steps of annealing we carried out, the more the minor peaks appeared and the stronger the higher minor peaks became. Combining with the results by DSC, SAXS, and WAXD measurements (see Figs. 8 and 10 and Table V), we suggested that the lamellar insertion occurred during the post-annealing of the crystallized sample. The SAXS results showed that the long periods decreased with the post-annealing at lower temperatures, which should demonstrate that some lamellae insertion occurred during post-annealing. It is clear that the minor lower melting peaks were associated to melting of the metastable crystal lamellae and that multiple lamellae thickness are more likely responsible for the multiple minor endothermic peaks.

CONCLUSION

In the crystallization or annealing process of polymers, crystal populations with various thickness and different metastability may be produced. The multiple melting phenomenon of PA1010 observed during DSC heating scans was attributed to the melting of metastable lamellae of different thickness. The upper endothermic peak was due to the melting of main lamellae with larger thickness, and the lower minor endothermic peaks were associated to the melting of thinner lamellae. Upon crystallization at an isothermal temperature, the thicker main crystal lamellae with the highest melting temperature was always the first formed, and the thinner lamellae started to develop at the stage when the growth of the main lamellae was close to completion. Compared with the thicker main lamellae, the thinner lamellae with lower melting temperature was metastable and could melt before the melting of thicker main lamellae.

Financial support was provided by the National Natural Science Foundation of China and the National Key Projects for Fundamental Research, Macromolecular Condensed State of the State Science and Technology Commission of China. Thanks also to Dr. B. Li for providing the PA sample.

REFERENCES

1. Mo, Z.; Meng, Q.; Feng, J.; Zhang, H.; Chen, D. Polym Int 1993, 32, 53.
2. Blundell, D. J.; Osborn, B. N. Polymer 1983, 24, 953.
3. Zachmann, H. G.; Stuart, H. A. Makromol Chem 1960, 41, 148.
4. Cebe, P.; Hong, S.-D. Polymer 1986, 27, 1183.
5. Cheng, S. Z. D.; Cao, M.-Y.; Wunderlich, B. Macromolecules 1986, 19, 1868.
6. Blundell, D. J. Polymer 1987, 28, 2248.
7. Tan, S.; Su, A.; Li, W.; Zhou, E. Macromol Rapid Commun 1998, 19, 11.
8. Tan, S.; Su, A.; Luo, J.; Zhou, E. Polymer 1999, 40, 1223.
9. Holdsworth, P. J.; Turner–Jones, A. Polymer 1970, 12, 195.
10. Strobl, G. R. Acta Crystallogr, Sect A 1970, 26, 367.
11. Bell, J. P.; Murayama, T. J Polym Sci A-2 1969, 7, 1059.
12. Roberts, R. C. Polymer 1969, 10, 117.
13. Bassett, D. C.; Olley, R. H.; Al Raheil, I. A. M. Polymer 1988, 29, 1745.
14. Hsiao, B. S.; Verma, R. K. Trends Polym Sci 1996, 4, 312.
15. Wunderlich, B. Thermal Analysis; Academic Press: New York, 1990.
16. Wunderlich, B. Macromolecular Physics, Vol. 2; Academic Press: New York, 1976.
17. Wunderlich, B. Macromolecular Physics, Vol. 3; Academic Press: New York, 1980.